Journal of Hard Tissue Biology 27[2] (2018) 147-154
2018 The Hard Tissue Biology Network Association
Printed in Japan, All rights reserved.
CODEN-JHTBFF, ISSN 1341-7649

Original

Bone Response to Nano-apatite Paste Derived from Ca-amino Acid Complex

Takuya Waki[1)], Chihiro Mochizuki[2)], Mitsunobu Sato[3)], Toshitsugu Sakurai[1)], Tohru Hayakawa[4)] and Chikahiro Ohkubo[1)]

[1)] *Department of Removable Prosthodontics, Tsurumi University School of Dental Medicine, Yokohama, Japan*
[2)] *Center for Promotion of Higher Education, Kogakuin University, Tokyo, Japan*
[3)] *Department of Applied Physics, School of Advanced Engineering, Kogakuin University, Tokyo, Japan*
[4)] *Department of Dental Engineering, Tsurumi University School of Dental Medicine, Yokohama, Japan*
(Accepted for publication, January 12, 2018)

Abstract: Nano-apatite could be prepared from a homogeneous solution of calcium (Ca)-aspartic acid (Asp) and Ca-glutamic acid (Glu) chelate complex with a high yield. Asp and Glu are components of non-collagenous proteins. Arginine is used to adjust pH to obtain precipitation from a Ca complex solution. Apatite from a Ca- ethylenediaminetetraacetic acid (EDTA) chelate complex was also prepared. These apatites are referred to as Asp-HA, Glu-HA, and EDTA-HA, respectively. Nano-apatite paste was obtained after mixing with water. Synthesized nano-apatite was characterized by X-ray diffraction and Fourier transform infrared measurements. It was revealed that Asp-HA and Glu-HA showed smaller crystal sizes with nano-scale, higher lattice distortion and greater degree of consistency as compared to EDTA-HA. The elution of Ca ion forms Asp-HA and Glu-HA were smaller than that of EDTA-HA. To investigate the influence of the different amino acid ligands for calcium on bone response, bone responses to each nano-apatite paste were evaluated after transplantation into the subperiosteal pocket of the rat calvarial skeleton. Asp-HA and Glu-HA showed greater amounts of new bone formation than EDTA-HA. New bone formation progressed at an especially early stage after implantation with Asp-HA. It is suggested that Asp-HA paste will be useful for bone regeneration.

Key words: Apatite, Aspartic acid, Glutamic acid, Calcium chelate complex, New bone formation

Introduction

Development of new bone reconstruction technique alternatives to autografts and allografts for bone reconstruction procedures is now required in dental clinical situation. Effectiveness of bone block allograft material or macroporous cellulose-based materials on bone regeneration has been reported[1,2)]. In addition, the application of recombinant bone morphogenetic protein type 2 (rhBMP-2) with absorbable material is also useful technique for bone reconstruction[3,4)]. Hydroxyapatite, with a chemical composition comparable to the mineral components of natural bone, is now widely used for bone substitutes or bone regeneration material due to its excellent biocompatibility and osteoconductivity[5-9)]. Various methods for preparing apatite include wet methods[10-12)], solid phase methods[13)], and hydrothermal methods[14,15)]. Wet methods are popular but take a long time and need careful pH control during the reaction.

Mochizuki *et al*. synthesized apatite with a different crystallinity from calcium (Ca)-ethylenediaminetetraacetic acid (EDTA) chelate complexes[16)]. This method was employed in a homogeneous solution of phosphoric acid, Ca-EDTA complex, H_2O_2, and NH_4OH. Apatite with different crystallinity was obtained by changing the heat condition and molar ratio of H_2O_2 to Ca. Hayakawa *et al*. prepared composites of poly(lactide-co-glycolide) (PLGA) and two types of apatite derived from Ca-EDTA with different crystallinities and evaluated their bone response by implantation experiments into cortical bone defects in rabbits[17,18)]. They concluded that more new bone formation was obtained using apatite with low crystallinity. They speculated that the greater degree of calcium ion dissolution from apatite with low crystallinity stimulated the activity of osteoblast cells and enhanced bone formation.

The advantages of apatite synthesis through the Ca-EDTA complex are that 1) the reaction mixture is a homogeneous solution, and the composition of the obtained apatite is also homogenous and that 2) it is easy to control the Ca/P ratio and apatite crystallinity by regulating the reaction conditions. However, lower crystallinity apatite from the Ca-EDTA complex is calcium-deficient apatite which Ca/P ratio is less than 1.67, a large amount of H_2O_2 is needed for the decomposition of the Ca-EDTA complex, and the yield of calcium-deficient apatite is very low, approximately 30%. For example, the yield of apatite synthesized by wet methods is approximately 70-80 %. The stability constant of the Ca complex will affect the decomposition of the complex and the yield. A lower stability constant will be produce easier decomposition of the Ca complex.

Iminodiacetic acid (IDA) is a one-end unit of EDTA, and L-aspartic acid (Asp) is an isomer of IDA. Both compounds form a chelate complex with the same metal ions as EDTA, and the stability constants of the Ca complex are lower than that of EDTA. The stability constants of Ca-IDA and Ca-Asp complexes are approximately 2.6 and 1.7, respectively, and that of the Ca-EDTA complex is approximately 10.6. Apatite with a different crystallinity could be prepared without the addition of H_2O_2 with a yield of approximately 80% from a Ca-IDA or Ca-Asp complex[19)]. However, no distinct differences were observed in bone responses toward PLGA/apatite composites from a Ca-IDA and Ca-Asp complex. It is suggested that the degradation of PLGA in the PLGA/apatite composite influenced new bone formation in addition to releasing and dissolving calcium from apatite.

Asp is one of the acidic amino acids constituting non-collagenous proteins. Non-collagenous proteins play a significant role in the calcification of hard tissue, such as bone or tooth[20,21)]. Some acidic amino acids, such as Asp or L-glutamine acid (Glu), are known to

Correspondence to: Dr. Takuya Waki, Department of Removable Prosthodontics, Tsurumi University School of Dental Medicine, 2-1-3, Tsurumi, Yokohama, Kanagawa 230-8501, Japan; TEL: +81-45580-8420; E-mail: waki-takuya@tsurumi-u.ac.jp

be components of osteocalcin or osteopontin, which promotes the remineralization of biological hard tissue[20].

It was found that apatite from the Ca-Asp complex could be formed in a paste after mixing with water. Acidic amino acids can form a chelate compound with Ca ions. This formative consistency of the apatite would contribute to the appropriate bone augmentation during implant placement procedures. In the present study, we aimed to investigate the influences of acidic amino acid ligands for calcium complexes on bone formation. Apatite from Asp and Glu was prepared, and new bone formation toward each apatite paste was evaluated after implantation into a subperiosteal pocket of rat calvaria. L-arginine (Arg) was used to adjust the pH to obtain precipitation from the Ca complex solution.

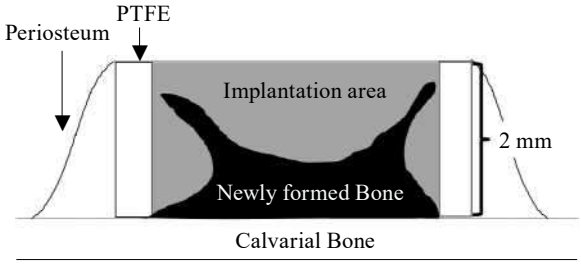

Figure 1. Schematic illustration for the implantation of PTFE tube (inside diameter of 3 mm, outer diameter of 4 mm, and height of 2 mm) containing apatite paste into periosteum pockets of rat calvaria. Apatite paste was filled into PTFE tube, and then PTFE tube was placed into the space between the periosteum and the calvarial bone surface of rats

Materials and Methods

Materials

L-aspartic acid (> 99.0%, Asp, Kanto Chemical Co., Inc., Tokyo, Japan), L-glutamic acid (> 99.0%, Glu, Wako Pure Chemical Industries, Ltd., Osaka, Japan), calcium hydroxide (> 99.9%, $Ca(OH)_2$, Wako Pure Chemical Industries, Ltd., Osaka, Japan), calcium acetate monohydrate (> 99.0%, $Ca(CH_3COO)_2 \cdot H_2O$, Kanto Chemical Co. Inc., Tokyo, Japan.), phosphoric acid (85%, H_3PO_4, Taisei Chemical Co., Ltd., Tokyo, Japan), L-arginine (> 98.0%, Arg, Wako Pure Chemical Industries, Ltd., Osaka, Japan.), and ammonium hydroxide (28%, NH_4OH, Taisei Chemical Co., Ltd., Tokyo, Japan.) were used as received materials in this study. LaB6 powder (NIST, USA) was employed to obtain the calibration curve for measuring the crystallite size by X-ray diffraction (XRD) measurement.

Synthesis of HA derived from a Ca-amino acid complex

Amino acid, L-Asp (3.99 g, 3 mmol) or L-Glu (4.41 g, 30 mmol), and $Ca(OH)_2$ (1.11 g, 15 mmol) were mixed in 300 ml of aqueous solution. The mixed solution was stirred in an ultrasonic bath below 5ºC for 60 min, and a homogeneous Ca-Asp or Ca-Glu solution was obtained. The clear solution was stirred at 60°C for 1 hour after cooling the solution at 37°C, and 85% H_3PO_4 (1.04 g, 9.0 mmol) was added to the Ca-Asp or Ca-Glu solution at room temperature. The Ca/P ratio was adjusted to the stoichiometric value of hydroxyapatite (1.67). The pH value of the clear solution was approximately 4.2 for Ca-Asp and 4.4 for Ca-Glu complex solutions. After the addition of Arg (10.5 g, 60 mmol) aqueous solution to the reaction mixture, white powders were immediately precipitated. The precipitates were collected on a paper filter. The pH value of the filtrate after removal of the precipitates was approximately 8.7 for Ca-Asp and 8.4 for Ca-Glu solutions. The white powders collected were dried overnight at 70°C. Apatites from the Ca-Asp and Ca-Glu complexes were obtained. The yields of Asp-HA and Ca-Glu were approximately 83% and 80%, respectively. Apatite with low crystallinity from the Ca-EDTA complex was also prepared according to the method of the previous reports[16]. These apatites are referred to as Asp-HA, Glu-HA, and EDTA-HA, respectively. NH_4OH was used as a basic reagent for precipitating apatite powder in EDTA-HA synthesis. Thus, three kinds of apatite Asp-HA, Glu-HA, and EDTA-HA were employed in the present study.

Apatite characterizations

The crystal structures and crystallite sizes of the apatites were characterized by XRD (SmartLab, Rigaku, Tokyo, Japan) measurement. The θ–2θ scan mode was employed with a Cu-Kα X-ray source at 45 kV and 200 mA. The crystallite sizes in these samples were obtained by the whole powder pattern fitting (WPPF) method[21], a numerical program based on the Rietveld method. LaB6 powder was used to obtain the calibration curve.

Fourier transform infrared (FT-IR) spectra were measured in transmission mode for the KBr-diluted discs at a constant resolution of 4 cm^{-1} and a range of 4000-100 cm^{-1} on an FT-IR-600 spectrophotometer (JASCO, Tokyo, Japan). The surface appearances and shapes of apatite were observed using a scanning electron microscope (JSM5600LV, JEOL Ltd., Tokyo, Japan) at an accelerating voltage of 10 kV.

Measurement of Ca ions eluted from apatite

Each apatite powder (20 mg) was immersed in double-distilled water (20 ml). The elution of Ca ions was monitored using a Ca ion measuring instrument (perfectIONTM, Mettler-Toledo AG, Schwerzenbach, Switzerland). The apatite suspension was vibrated for 1 min and maintained at 37°C during the measurement. The elution of Ca ions was measured after 1, 3, 7, 14, 21, and 28 days of immersion. Three runs for measurements were performed for each apatite.

Measuring the consistency of apatite paste

The consistency of apatite paste was measured according to the methods of the previous report by Shinozaki[22], with a slight modification. Apatite powder 100 mg was kneaded into a paste with 70 µl of distilled water. Immediately after the paste was made, it was filled into a silicone mold (internal diameter of 10 mm and height of 0.5 mm) on a polyethylene terephthalate (PTFE) plate. The top surface of the apatite paste was covered by a PTFE plate to flatten it, and the covered PTFE plate was then removed. After carefully removing the bottom PTFE plate and silicone mold, apatite disks were used to measure the consistency. The apatite paste disk was placed on a glass plate, and another glass plate was then carefully placed on another surface of the apatite paste disk. The assembly was placed on the surface of a metal disk in a constant load compression testing machine (A-001 Japan Mecc Co. Ltd., Tokyo, Japan) for loading. The apatite paste disk was loaded continuously at 2 MPa at 20°C for 10 min. The diameter of the spread disk was measured with calipers (accuracy: 50 µm).

Implantation procedure

The animal study was conducted in accordance with the animal experiment ethical guidelines of Tsurumi University (Certificate Number: 27A051). Nine-week-old male Sprague Dawley rats (Japan SLC, Inc., Shizuoka, Japan) weighing 270-370 g were used. The rats were kept under a standard light-dark schedule with a 12-h interval, relative humidity of 60 ± 10%, and a temperature of 23 ± 1ºC. Stock diet (CE-2, Nippon Formula Feed Manufacturing Co., Ltd., Yokohama, Japan) and tap water were available ad libitum. As shown in Fig.1,

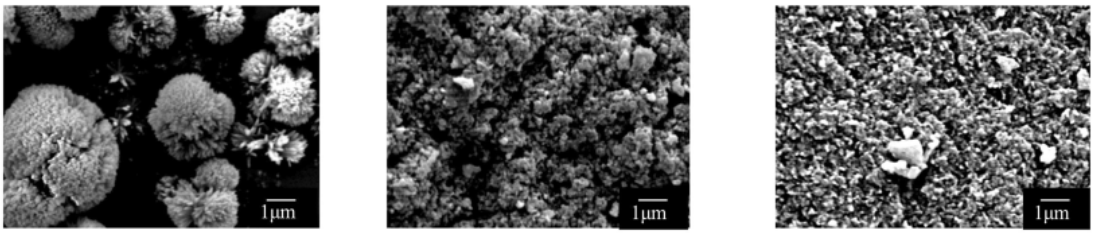

Figure 2. SEM images of apatite derived from Ca chelate complexes of (a) EDTA-HA, (b) Asp-HA, (c) Glu-HA.
Asp-HA and Glu-HA crystals were finer than those of EDTA-HA. EDTA-HA had a globular structure with needle-like crystals.

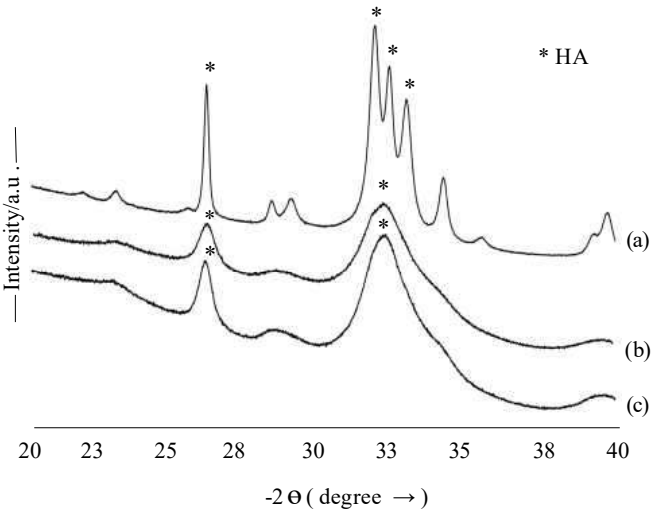

Figure 3. XRD patterns of apatite derived from Ca chelate complexes of (a) EDTA-HA, (b) Asp-HA, (c) Glu-HA.
Asp-HA and Glu-HA showed broader patterns than EDTA-HA. Broad peaks of apatite could be observed at around 2θ = 26, 32–33°. For EDTA-HA, three sharp peaks derived from apatite were identified at 2θ = 31.76, 32.26, and 32.83°.

apatite pastes from EDTA-HA, Asp-HA, and Glu-HA were inserted into the space between the periosteum and the calvarial bone of rats in accordance with the procedure established in previous reports[23-25].

Each animal received one material. Twenty-four apatite pastes were divided into six groups, namely three kinds of apatite paste EDTA-HA, Asp-HA, and Glu-HA and two implantation periods 4 weeks and 8 weeks. Before surgery, all apatite and PTFE rings were sterilized with ethylene-oxide gas. Surgery was performed under general inhalation anesthesia with a 4% isoflurane (Forane, Abbott Japan Co., Ltd., Tokyo, Japan) and oxygen mixture, which was reduced to 2% isoflurane during surgical manipulation. Local anesthesia was performed by the injection of xylocaine. To reduce the perioperative infection risk, a prophylactic antibiotic, Shiomalim (equivalent to Latamoxef sodium, Shionogi & Co. Ltd., Osaka, Japan), was administered postoperatively by subcutaneous injection. The heads of the rats were shaved and disinfected with iodine tincture.

Apatite paste was filled into a PTFE tube. This cylindrical tube had an inside diameter of 3 mm, outer diameter of 4 mm, and height of 2 mm. After elevating the full-thickness epidermis, hypodermal tissue, and periosteal flaps, PEFE tubes filled with paste were placed directly on the calvarial bone surface. The decortication of calvarial bone was not performed prior insert the materials. After placing PTFE tubes into the pocket, the periosteal flap was returned and sutured over the surface of the implanted materials using nonabsorbable 4-0 nylon sutures. There was no injury to promote bleedings during the operation.

Micro-CT and histological observation

Four or 8 weeks after implantation, tissue specimens including PTFE tubes were dissected using a diamond saw (Cutting Grinding System, BS-300CP band system, EXAKT, Apparatebau GmbH & Co., KG, Norderstedt, Germany). Specimens were fixed in 10% neutral buffered formalin for 7 days and then were dehydrated through a graded series of ethanol (70%, 80%, 90%, 96%, and 100%). Newly formed bone inside the PTFE tube was first observed using high-resolution microfocus X-ray computed tomography (micro-CT, inspeXio, Shimadzu, Kyoto, Japan) with a voltage of 115 kV and a current of 70 μA. An isotropic resolution of 32 μm/voxel was selected, which displayed the microstructure of the rat's calvarial bone. The original three-dimensional (3D) images were displayed and analyzed with software (TRI/3D-BON-FCS64, RATOC System Engineering, Co., Ltd., Tokyo, Japan). After micro-CT observation, CT values were converted to brightness values. New bone formation was determined based on the brightness histogram. The brightness of newly formed bone was almost the same as that of calvaria bone.

After micro-CT observation, the specimens were embedded in methyl methacrylate resin. After polymerization at 37°C, non-decalcified thin sections were prepared using a cutting-grinding technique (EXAKT-Cutting Grinding System, BS-300CP band system & 400CS microgrinding system; EXAKT Apparatebau, Norderstedt, Germany)[26]. Sections approximately 60 to 80 μm thick were obtained. One or two sections at the middle part of the implant materials were obtained from each apatite specimen. Sections were stained with methylene blue and basic fuchsin.

New bone formation in PTFE tubes was evaluated using a light microscope (Eclipse Ni, Nikon, Tokyo, Japan; magnification ×100). In addition to a descriptive evaluation, histomorphometrical analysis was performed on new bone formation. The area of newly formed bone in a PTFE tube was analyzed as newly formed bone mass (BM) using an image analysis system (WinROOF, Visual System Division, Mitani Corp., Tokyo, Japan). BM was defined as the percentage of the area of newly formed bone to the entire area inside the PTFE tube.

Statistical analysis

Data regarding the consistency, amount of Ca ions eluted, and BM of the three kinds of apatite were evaluated by one-way analysis of variance (ANOVA) using Origin Pro 9.0J (OriginLab Corp., Northampton, MA, USA) and Tukey's test for multiple comparisons among means. The data for bone mass between 4 weeks and 8 weeks for each apatite group were analyzed by unpaired *t*-test. P values of less than 0.05 were considered significant, and data were expressed as the mean ± standard deviation (SD).

Table 1. Crystallite size and lattice distortion of apatite examined by XRD

Apatite	EDTA-HA	Asp-HA	Glu-HA
Crystallite size (nm)	50.63 (3.2)	14.82 (0.93)	10.09 (0.19)
Lattice distortion (%)	0.379 (0.008)	0.756 (0.028)	0.975 (0.083)

( ): SD, n=3

Table 2. Consistency of the paste of kneaded apatite powder and distilled water

Apatite	EDTA-HA	Asp-HA	Glu-HA
Consistency (cm)	6.5 (0.2)[a]	8.9 (0.8)	10.3 (1.5)[b]

( ): SD, n=3

Different letters indicate no significant differences in the same row (p <0.05)

Table 3. Percentage of measured bone mass by micro-CT

Apatite	EDTA-HA	Asp-HA	Glu-HA
4 weeks	10.3 (2.0)[a,A]	17.9 (4.7)[b,A]	6.2 (1.8)[a,A]
8 weeks	20.3 (8.1)[b,B]	36.7 (8.8)[a,B]	35.3 (2.2)[a,B]

( ): SD, n=4

Different small letters indicate significant differences among the three kinds of apatite at 4 weeks and at 8 weeks in the same row (p <0.05).

Table 4. Percentage of measured bone mass (%)

Apatite	EDTA-HA	Asp-HA	Glu-HA
4 weeks	9.1 (3.2)[a, A]	20.5 (4.3)[b, A]	9.1 (0.2)[a, A]
8 weeks	18.4 (5.5)[b, B]	28.6 (10.0)[a, B]	28.3 (9.0)[a, B]

( ): SD, n=4

Different small letters indicate significant differences among the three kinds of apatite at 4 weeks and at 8 weeks in the same row (p <0.05).

Different large letters indicate significant differences between 4 weeks and 8 weeks in the same column (p <0.05).

Results

Apatite characterization

Fig. 2 shows SEM pictures of three apatite powders. Asp-HA and Glu-HA crystals were finer than those of EDTA-HA. EDTA-HA had a globular structure with needle-like crystals.

Fig. 3 shows the XRD patterns of three kinds of apatite. Asp-HA and Glu-HA showed broader patterns than EDTA-HA. Broad peaks of apatite could be observed at around 2θ = 26, 32–33°. For EDTA-HA, three sharp peaks derived from apatite were identified at 2θ = 31.76, 32.26, and 32.83°. The crystallite size and lattice distortion of the different apatites are shown in Table 1. The crystal sizes of Asp-HA and Glu-HA were smaller than that of EDTA-HA. The lattice distortions of Glu-HA and Asp-HA were higher than that of EDTA-HA.

Fig. 4 shows the FT-IR spectra of three kinds of apatite. The peaks derived from phosphate groups were observed at around 962, 1036, 1095 cm^{-1}, and 565–601 cm^{-1}; peaks from carbonate ions were also observed at around 865, 1350, 1413, and 1633 cm^{-1} for the three kinds of apatite. It was revealed that the obtained apatite was a B-type carbonate apatite[27]. More carbonate ions were recognized for Asp-HA. The incorporation of amino acids was confirmed for Asp-HA and Glu-HA by peaks derived from the carboxyl group at around 1350 cm^{-1} and broad peaks derived from amino groups at around 3200-3400 cm^{-1}.

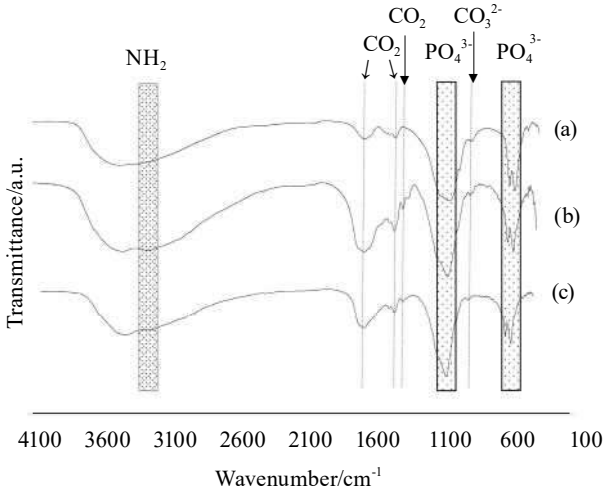

Figure 4. FT-IR spectra of apatite derived from Ca chelate complexes of (a) EDTA-HA, (b) Asp-HA, (c) Glu-HA.
The peaks derived from phosphate groups were observed at around 962, 1036, 1095 cm^{-1}, and 565–601 cm^{-1}; peaks from carbonate ions were also observed at around 865, 1350, 1413, and 1633 cm^{-1} for the three kinds of apatite. Broad peaks derived from amino groups at around 3200-3400 cm^{-1}.

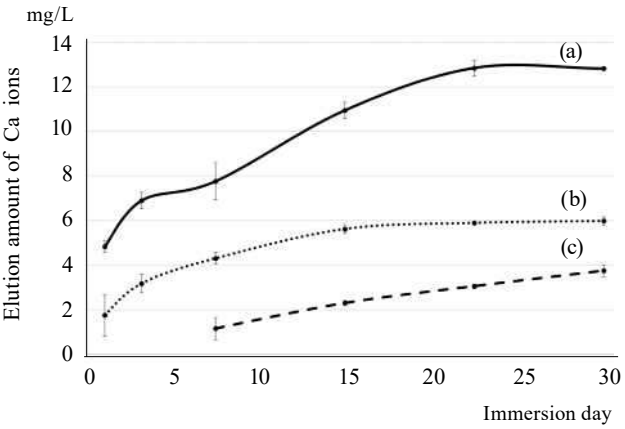

Figure 5. Elution amounts of Ca ions from apatite of (a) EDTA-HA, (b) Asp-HA, (c) Glu-HA.
The amount of calcium ions eluted from EDTA-HA was highest, and that from Glu-HA was lowest among three apatites (p < 0.05). After 21 days of immersion, the elution of Ca ions was almost constant.

Elution of Ca ions

The amounts of eluted Ca ions from three different apatites are shown in Fig. 5. At day 0, the amount of elution was very low and under the detection limit. At days 1 and 3 of immersion, elution from Glu-HA was not still detectable. The amount of calcium ions eluted from EDTA-HA was highest, and that from Glu-HA was lowest among three apatites (p < 0.05). After 21 days of immersion, the elution of Ca ions was almost constant, and there was no significant increase in the three different apatites.

Consistency of the apatite paste

The results of the diameter of a paste disk after loading were listed in Table 2. There was a significant difference in the diameter between EDTA-HA and Glu-HA (p < 0.05). No significant difference existed between EDTA-HA and Asp-HA or between Asp-HA and Glu-HA.

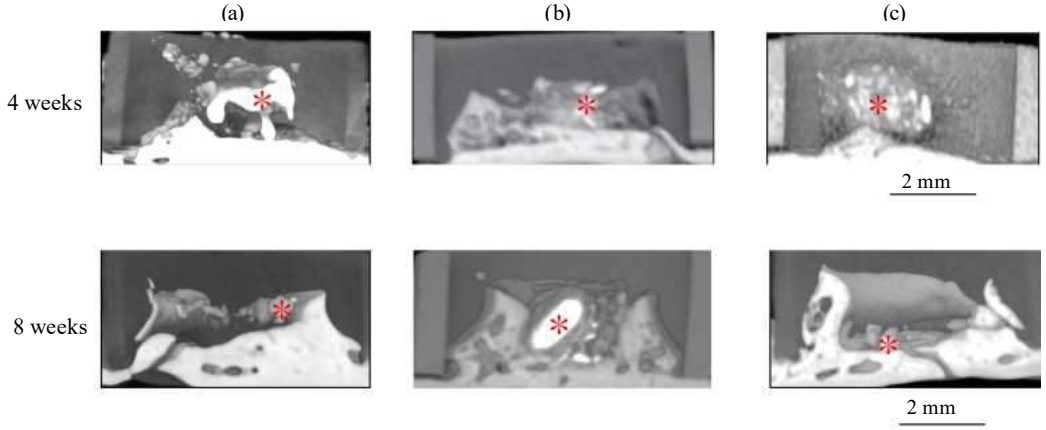

Figure 6. Three-dimensional CT images of newly formed bone inside PTFE tubes of (a) EDTA-HA, (b) Asp-HA, (c) Glu-HA. Asterisk: residual apatite.
New bone formation was clearly observed for Asp-HA at 4 weeks. For Glu-HA, slight new bone formation was also recognized. At 8 weeks, new bone formation was identified for three different apatites. Especially Asp-HA and Glu-HA showed greater amounts of new bone formation.

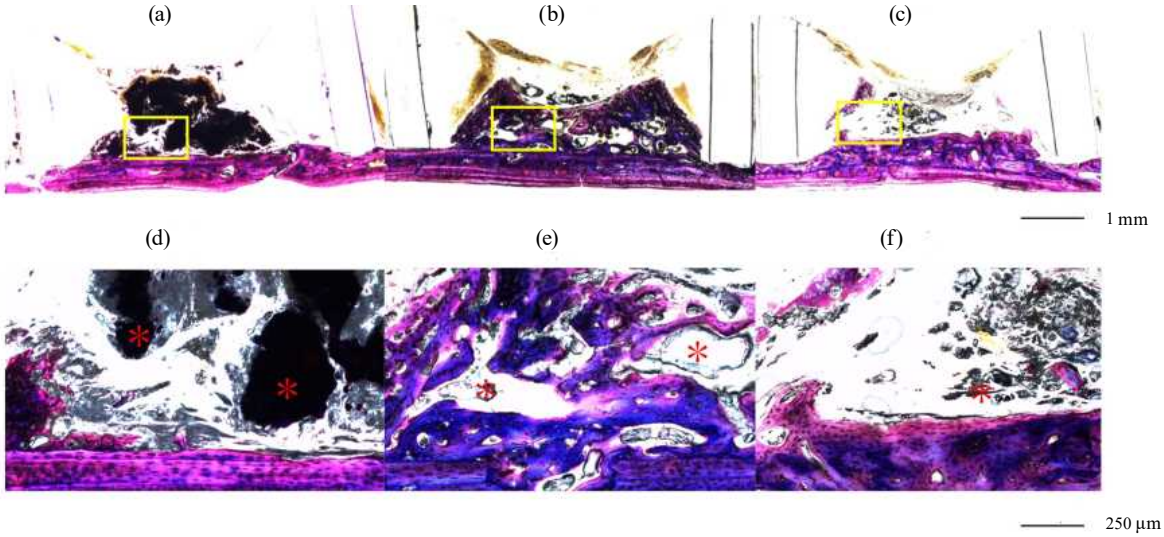

Figure 7. Histological appearances of newly formed bone inside PTFE tubes of (a), (d) EDTA-HA, (b), (e) Asp-HA, (c), (f) Glu-HA 4 weeks after surgery. (d), (e) and (d) are higher magnification images of the boxed area in (a), (b) and (c), respectively. Asterisk:residual apatite.

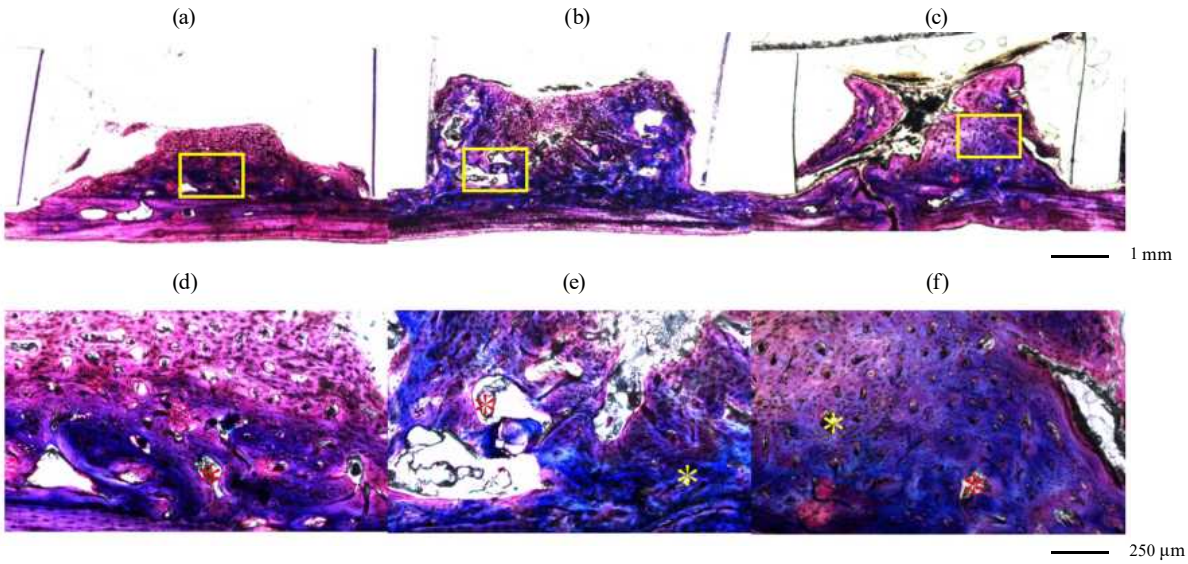

Figure 8. Histological appearances of newly formed bone inside PTFE tubes of (a), (d) EDTA-HA, (b), (e) Asp-HA, (c), (f) Glu-HA 8 weeks after surgery. (d), (e) and (d) are higher magnification images of the boxed area in (a), (b) and (c), respectively. Asterisk: residual apatite. Arrow head: Haversian canal.
In (d), formation of external circumferential lamella was observed, and in (e) and (f) presence of Haversian canal was identified.

Micro-CT observation

Fig. 6 shows the micro-CT images of newly formed bone in the PTFE tubes at 4 and 8 weeks. For EDTA-HA at 4 weeks, newly formed bone could not be clearly observed, and much residual apatite was recognized. On the contrary, new bone formation was clearly observed for Asp-HA at 4 weeks. For Glu-HA, slight new bone formation was also recognized at 4 weeks. At 8 weeks, new bone formation was identified for three different apatites. Especially Asp-HA and Glu-HA showed greater amounts of new bone formation. In all groups, new bone formation could be observed from the calvarial side but not from the periosteum side.

Quantification of BM from micro-CT images were shown in Table 3. BM value of Asp-HA was significantly higher than those of EDTA-HA and Glu-HA ($p < 0.05$) after the 4 weeks of the implantation. No significant difference in BM was observed between EDTA-HA and Glu-HA. At 8 weeks, Asp-HA and Glu-HA showed significantly greater BM values than EDTA-HA ($p < 0.05$). No significant differences were existed in the BM of Asp-HA and Glu-HA. Comparing 4 and 8 weeks for three different apatites, significant increase of BM values were recognized ($p < 0.05$).

Histological observation

The histological appearances of three different apatites at 4 and 8 weeks are shown in Fig. 7, 8. No clear signs of an inflammatory response were observed in any specimen. The histological appearances corresponded with the results of micro-CT observation. New bone formation was observed from the calvarial side but not from the periosteum side for different apatite specimens. At 4 weeks, no clear formation of new bone was recognized, and residual apatite was clearly identified for EDTA-HA. More new bone formation was observed for Asp-HA.

At 8 weeks, more new bone formation could be observed in three different groups as compared to 4 weeks. EDTA-HA showed new bone formation with external circumferential lamella, and no clear apatite residue was recognized. Asp-HA and Glu-HA specimens showed more new bone formation than did EDT-HA. Presence of Haversian canal was identified as shown in Fig 8e and 8f (arrow head). Slight apatite residue was recognized for the Glu-HA specimen.

BM measurements are listed in Table 4. Results were almost the same in the results from micro-CT images. But more accurate BM values were obtained from histomorphometrical analysis. At 4 weeks, the BM value of Asp-HA was significantly higher than those of EDTA-HA and Glu-HA ($p < 0.05$). No significant difference in BM was observed between EDTA-HA and Glu-HA. At 8weeks, the BM values of Asp-HA and Glu-HA were significantly greater than that of EDTA-HA ($p < 0.05$). There were no significant differences in the BM of Asp-HA and Glu-HA. BM values significantly increased from 4 to 8 weeks for three different apatites ($p < 0.05$).

Discussion

In the present study, apatite could be prepared from Ca-acidic amino acid complexes. As acidic amino acids, Asp and Glu were selected. Both are components of non-collagenous proteins. Apatite from a Ca-EDTA complex was also prepared. New bone formation toward apatite paste was evaluated after implantation into a subperiosteal pocket of rat calvaria. This revealed that new bone formation was influenced by the differences in acidic amino acids as a ligand of the Ca complex, and new bone formation progressed in apatite from the Ca-Asp complex at an early stage.

Various kinds of bone grafts materials for bone reconstruction are now reported. In addition, the combination of rhBMP with absorbable material is an effective technique[28,29]. It is well known that BMP can accelerate not only bone formation. Chitosan/nano-hydroxyapatite microspheres or nano-hydroxyapatite and silk fibroin composites are reported to be candidates as scaffolds for bone tissue engineering[30,31].

There were a few reports for bone augmentation using subperiosteal pocket model of rat calvaria. Matsui *et al*. reported that calvarial augmentation was enhanced by the implantation of octacalcium phosphate-collagen composites if suitable mechanical stress were provided[23]. Den *et al*. demonstrated the difference of bone augmentation between absorbable and nonabsorbable interconnected porous apatites after the implantation into the subperiosteal pocket of rat calvaria[24]. New bone formation was observed from the calvarial surface, not from the periostum like the present experiment.

Acidic amino acids in non-collagen proteins influence biological mineralization. It is well known that Asp-rich sequences are contained in dentin phosphoprotein and osteopontin, and Glu-rich sequences are in osteonectin and bone sialoprotein[32,33]. Asp and Glu are more highly expressed in the family of small integrin-binding ligand, N-linked glycoproteins (SIBLINGs), which is known to play a key role in apatite mineralization in the body[34]. SIBLINGs also contain positively charged Arg. Moreover, Glu enhanced the differentiation of osteoblast cells and inhibits the differentiation of osteoclast cells[35-37]. It has been reported that acidic amino acids such as Asp and Glu bind to apatite due to their electric charges[38]. Thus, Asp-HA and Glu-HA include Asp and Glu, respectively, as revealed by FT-IR measurement, although no quantitative data for incorporating amino acids was obtained.

In a previous experiment, NH_4OH was used as basic reagent for obtaining the precipitation of apatite from the Ca-EDTA complex homogeneous solution[16]. As a result, the ammonium salt of EDTA was incorporated into the EDTA-HA powder. Apatite formation in gelatin gel from the Ca-Asp complex was reported when Arg was added[39]. Arg is a basic amino acid and also a component of non-collagen proteins. It has been reported that Arg could potentially increase bone formation over bone resorption and, consequently, increase bone mass[40]. Thus, Arg is used as a basic reagent for preparing Asp-HA and Glu-HA.

Asp-HA and Glu-HA showed smaller crystal sizes and higher lattice distortion as compared to EDTA-HA. Both are nanostructured apatites. The present homogeneous solution method, starting from a Ca chelate complex, can easily produce nanoscale apatites with high yields. Generally, apatite with lower degrees of crystallinity will cause higher amount of Ca ion elution. In the present study, EDTA-HA showed higher crystallinity than Asp-HA and Glu-HA. However, EDTA-HA showed greater value of the Ca ion elution than Asp-HA and Glu-HA. The reason is still not clear, but it is presumed that the carbonate content in apatite and the crystal size influenced the elution of Ca ions. The present three apatites were carbonate apatites. It has been reported that the carbonate ion content in apatites influences their degradation behavior[41]. The presence of more carbonate ions causes easier and earlier decomposition of apatite. FT-IR measurements indicated that more carbonate ions are incorporated into Asp-HA than Glu-HA and EDTA-HA, and the order according to carbonate ion content is Asp-HA, Glu-HA, and EDTA-HA. The order of the elution of Ca ions is reversed, namely, EDTA-HA, Asp-HA, and Glu-HA. The content ratio of carbonate ions in apatite should be further investigated and analyzed in detail.

EDTA-HA showed no new bone formation at an early stage regardless of the greater amount of Ca ion elution. On the other hand, Asp-HA showed less Ca ion elution but more new bone formation. As mentioned above, the present Asp-HA and Glu-HA were nanoscale

apatites. Some have reported the effectiveness of nanoscale apatites for bone regeneration or mineralization[8,42,43]. Zhu *et al*. reported that nanophase apatite artificial bone stimulated a callus that was bonier than those of microphase apatites[44]. Smaller apatite particles more closely resemble the characteristics of natural apatite during biomineralization than do larger apatite particles. Nanophase apatite may encourage osteoblast adhesion, proliferation, and, eventually, rapid repair of hard tissue injuries[45]. Thus, it is speculated that the present nanoscale Asp-HA and Glu-HA are more effective for new bone formation than macro-scale EDTA-HA, according to the previous reports.

Asp-HA and Glu-HA contained each amino acid. Thus, the incorporation of amino acids Asp and Glu into Asp-HA and Glu-HA also will influence new bone formation. Besides acidic amino acids, phosphorylated proteins in non-collagenous protein played a key role in controlling mineralization[34]. Jahromi *et al*. insisted that contradictory results were reported by different authors about the effect of apatite particle growth[38]. The *in vivo* bone formation needs more factors such as protein adsorption, cell activities etc. More studies including cell assay and /or animal implantation experiments should be needed.

Another reason for the delay of new bone formation for EDTA-HA is that the incorporation of the ammonium salt of EDTA will inhibit new bone formation. For Asp-HA and Glu-HA, Arg is incorporated into the apatite. Arg is also effective for new bone formation, as mentioned above. The reason of the difference in bone formation between Asp-HA and Glu-HA at an earlier stage is not clear. More detailed studies for elucidating earlier bone formation of Asp-HA should be further investigated.

In this study, apatite paste was applied inside the periosteum pocket on the calvaria. For bone augmentation, the formative consistency of HA paste would be helpful for bone defects of any shape. The efficacy of apatite paste in treating bone defects with a bone-healing process will be further elucidated. The viscosity of the present HA paste can be controlled by mixing only water without any reagents, and be prepared at a chair side in a short time. The present HA paste has a possibility to provide an easy and wide application in dental clinics. Besides Asp and Glu, HA synthesis from a Ca chelate complex with other amino acids such as glycine, serine, or peptides from Asp and/or Glu will be investigated in our next studies.

In conclusion, this study, apatite could be obtained from Ca-Asp and Ca-Glu chelate complexes with high yields and be formed as paste after mixing with water. The crystallographic character was analyzed, and the consistency, elution of Ca ions, and new bone formation of these apatites were investigated and compared with apatite from a Ca-EDTA complex. The obtained apatite contained carbonate. Asp-HA and Glu-HA showed smaller crystal sizes with nanoscale, higher lattice distortion and greater degrees of consistency as compared to EDTA-HA. Elution of Ca ions from Asp-HA and Glu-HA was smaller than that of EDTA-HA. Asp-HA and Glu-HA showed more new bone formation than did EDTA-HA. New bone formation progressed at an especially early stage for Asp-HA after implantation. It can be suggested that Asp-HA paste will be useful for bone regeneration.

Acknowledgments

This study was supported in part by Grants-in-Aid for Scientific Research (C) (17K11815) from the Japan Society for the Promotion of Science and by MEXT-Supported Program for Strategic Research Foundation at Private Universities, 2015–2019.

Conflicts of Interest

The authors declare no conflict of interest.

References

1. Laino L, Iezzi G, Piattelli A, Lo ML and Cicciù M. Vertical ridge augmentation of the atrophic posterior mandible with sandwich technique: bone block from the chin area versus corticocancellous bone block allograft--clinical and histological prospective randomized controlled study. Biomed Res Int 2014: 982104, 2014
2. Petrauskaite O, Gomes PS, Fernandes MH, Juodzbalys G, Stumbras A, Maminskas J, Liesiene J and Cicciù M. Biomimetic mineralization on a macroporous cellulose-based matrix for bone regeneration. Biomed Res Int 2013: 452750, 2013
3. Cicciù M, Herford AS, Cicciù D, Tandon R and Maiorana C. Recombinant human bone morphogenetic protein-2 promote and stabilize hard and soft tissue healing for large mandibular new bone reconstruction defects. J Craniofac Surg 25: 860-862, 2014
4. Cicciù M. Real opportunity for the present and a forward step for the future of bone tissue engineering. J Craniofac Surg 28: 592-593, 2017
5. LeGeros RZ. Properties of osteoconductive biomaterials: calcium phosphates. Clin Orthop Relat Res 395: 81–98, 2002
6. LeGeros RZ. Calcium phosphate-based osteoinductive materials. Chem Rev 108: 4742–4753, 2008
7. Vallet-Regí M and Ruiz-Hernández E. Bioceramics: from bone regeneration to cancer nanomedicine. Adv Mater 23: 5177–5218, 2011
8. Zakaria SM, Sharif Zein SH, Othman MR, Yang F and Jansen JA. Nanophase hydroxyapatite as a biomaterial in advanced hard tissue engineering: a review. Tissue Eng Part B Rev 19: 431–441, 2013
9. Bose S and Tarafder S. Apatite calcium phosphate ceramic systems in growth factor and drug delivery for bone tissue engineering: a review. Acta Biomater 8: 1401–1421, 2012
10. Rao RR, Roopa HN and Kannan TS. Solid state synthesis and thermal stability of HAP and HAP-β-TCP composite ceramic powders. J Mater Sci: Mater Med 8: 511–518, 1997
11. Tadic D, Peters F and Epple M. Continuous synthesis of amorphous carbonated apatites. Biomaterials 23: 2553–2559, 2002
12. Landi E, Tampieri A, Celotti G, Vichi L and Sandri M. Influence of synthesis and sintering parameters on the characteristics of carbonate apatite. Biomaterials 25: 1963–1770, 2004
13. Luo P and Nieh TG. Preparing hydroxyapatite powders with controlled morphology. Biomaterials 17: 1959–1964, 1996
14. Aizawa M, Porter AE, Best SM and Bonfield W. Ultrastructural observation of single-crystal apatite fibers. Biomaterials 26: 3427–3433, 2005
15. Saheb AM and Sedigheh J. Synthesis of hydroxyapatite nanostructure by hydrothermal condition for biomedical application. Iran J Pharm Sci 5: 89–94, 2007
16. Mochizuki C, Sasaki Y, Hara H, Sato M, Hayakawa T, Yang F, Hu X, Shen H and Wang S. Crystallinity control of apatite through Ca-EDTA complexes and porous composites with PLGA. J Biomed Mater Res B Appl Biomater 90: 290–301, 2009
17. Hayakawa T, Mochizuki C, Hara H, Fukushima T, Sato M, Yang F, Shen H and Wang S. Influence of apatite crystallinity in porous PLGA/apatite composite scaffold on cortical bone response. J Hard Tissue Biol 18: 7–12, 2009
18. Hayakawa T, Mochizuki C, Hara H, Yang F, Shen H, Wang S and Sato M. *In vivo* evaluation of composites of PLGA and apatite with two different levels of crystallinity. J Mater Sci: Mater in Med 21: 251–258, 2010
19. Hayakawa T, Mochizuki C, Hara H, Amemiya T, Hirayama S, Yang F, Shen H, Wang S, Hamada Y and Sato M. Cortical bone response

towards porous composites of PLGA and apatite prepared from calcium complexes. J Hard Tissue Biol 21: 345–350, 2012
20. Landis WJ and Jacquet R. Association of calcium and phosphate ions with collagen in the mineralization of vertebrate tissues. Calcified Tissue Int 93: 329–337, 2013
21. Toraya, H. Whole-powder-pattern fitting without reference to a structural model: application to X-ray powder diffraction data. J Appl Cryst 19: 440–447, 1986
22. Shinozaki Y, Mori N, Ohno J, Kawaguchi M, Kido H, Hayakawa T and Fukushima T. Rat calvarial tissues response to flowable DNA/protamine complex mixtures with DNA/chitosan complex to be used as a protective membrane for guided bone regeneration. J Oral Tissue Engin 9: 159–166, 2012
23. Matsui A, Anada T, Masuda T, Honda Y, Miyatake N, Kawai T, Kamakura S, Echigo S and Suzuki O. Mechanical stress-related calvaria bone augmentation by onlayed octacalcium phosphate–collagen implant. Tissue Eng Part A 16: 139–151, 2010
24. Den M, Amemiya T and Hayakawa H. Bone augmentation of interconnected porous calcium phosphates using periosteum elevation model on rat calvaria. J Jpn Soc Oral Implant 26: 433–443, 2013
25. Amemiya T, Fukayo Y, Nakaoka K, Hamada Y and Hayakawa T. Tissue response of surface modified three-dimensional titanium fiber structure. J Hard Tissue Biol 23: 137–148, 2014
26. Donath K and Breuner G. A method for study of undecalcified bones and teeth with attached soft tissues: the Sage-Schliff (sawing and grinding) technique. J Oral Pathol 11: 318–326, 1982
27. Layani JD, Mayer I and Cuisinier FJ. Carbonated hydroxyapatites precipitated in the presence of Ti. J Inorg Biochem 81: 57–63, 2000
28. Herford AS and Cicciù M. Recombinant human bone morphogenetic protein type 2 jaw reconstruction in patients affected by giant cell tumor. J Craniofac Surg 21: 1970-1975, 2010
29. Herford AS, Cicciù M, Eftimie LF, Miller M, Signorino F, Famà F, Cervino, Giudice G, Bramanti GL, Lauritano E, Troiano F, Muzio G and Laino LL. rhBMP-2 applied as support of distraction osteogenesis: a split-mouth histological study over nonhuman primates mandibles. Int J Clin Exp Med 9: 17187-17194, 2016
30. Chesnutt BM, Yuan Y, Buddington K, Haggard WO and Bumgardner JD. Composite chitosan/nano-hydroxyapatite scaffolds induce osteocalcin production by osteoblasts *in vitro* and support bone formation *in vivo*. Tissue Eng Part A 15: 2571-2579, 2009
31. Liu H, Xu GW, Wang YF, Zhao HS, Xiong S, Wu Y, Heng BC, An CR, Zhu GH and Xie DH. Composite scaffolds of nano-hydroxyapatite and silk fibroin enhance mesenchymal stem cell-based bone regeneration via the interleukin 1 alpha autocrine/paracrine signaling loop. Biomaterials 49: 103-112, 2015
32. Oldberg A, Franzén A and Heinegård D. Cloning and sequence analysis of rat bone sialoprotein (osteopontin) cDNA reveals an Arg-Gly-Asp cell-binding sequence. Proc Natl Acad Sci USA 83: 8819–8823, 1986
33. Oldberg A, Franzén A and Heinegård D. The primary structure of a cell-binding bone sialoprotein. J Biol Chem 263: 19430–19432, 1988
34. George A and Veis A. Phosphorylated proteins and control over apatite nucleation, crystal growth, and inhibition. Chem Rev 108: 4670–4693, 2008
35. Takarada T and Yoneda Y. Pharmacological topics of bone metabolism: glutamate as a signal mediator in bone. J Pharmacol Sci 106: 536–541, 2008
36. Hinoi E, Takarada T and Yoneda Y. Glutamate signaling system in bone. J Pharmacol Sci 94: 215–220, 2004
37. Hinoi E, Takarada T, Uno K, Inoue M, Murafuji Y and Yoneda Y. Glutamate suppresses osteoclastogenesis through the cystine/glutamate antiporter. Am J Pathol 170: 1277–1290, 2007
38. Jahromi MT, Yao G and Cerruti M. The importance of amino acid interactions in the crystallization of hydroxyapatite. J R Soc Interface 10: 20120906, 2013.
39. Hayakawa T, Mochizuki C, Amemiya T, Fukayo Y, Wada T, Ozawa D, Hamada Y, Sugawara Y and Sato M. Bone response of gelatin composite including the apatite prepared from an amino acid calcium complex. J Oral Tissue Engine 12: 115–120, 2015
40. Clementi G, Fiore CE, Mangano NG, Cutuli VM, Pennisi P, Caruso A, Prato A, Matera M and Amico-Roxas M. Role of soy diet and L-arginine in cyclosporin-A-induced osteopenia in rats. Pharmacol Toxicol 88: 16–19, 2001
41. LeGeros RZ and Tung MS. Chemical stability of carbonate- and fluoride-containing apatites. Caries Res 17: 419–429, 1983
42. Smith IO, McCabe LR and Baumann MJ. MC3T3-E1 osteoblast attachment and proliferation on porous hydroxyapatite scaffolds fabricated with nanophase powder. Int J Nanomedicine 1: 189–194, 2006
43. Balasundaram G, Satoa M and Webster TJ. Using hydroxyapatite nanoparticles and decreased crystallinity to promote osteoblast adhesion similar to functionalizing with RGD. Biomater 27: 2798–2805, 2006
44. Zhu W, Zhang X, Wang D, Lu W, Ou Y, Han Y, Zhou K, Liu H, Fen W, Peng L, He C and Zeng Y. Experimental study on the conduction function of nano-hydroxyapatite artificial bone. Micro Nano Lett 5: 19–27, 2010
45. Cerroni L, Filocamo R, Fabbri M, Piconi C, Caropreso S and Condò SG. Growth of osteoblast-like cells on porous hydroxyapatite ceramics: an *in vitro* study. Biomol Eng 19: 119–124, 2002